Anatomy of the thoracic paravertebral space: 3D micro-CT findings and their clinical implications for nerve blockade

Tae-Hyeon Cho,[1] Shin Hyung Kim ,[2] Jehoon O,[1] Hyun-Jin Kwon,[1] Ki Wook Kim ,[2] Hun-Mu Yang [1,3]

► Additional supplemental material is published online only. To view, please visit the journal online (http://dx.doi.org/10.1136/rapm-2021-102588).

[1]Department of Anatomy, Yonsei University College of Medicine, Seoul, Korea (the Republic of)
[2]Department of Anesthesiology and Pain Medicine, Yonsei University College of Medicine, Seoul, Korea (the Republic of)
[3]Surgical Anatomy Education Centre, Yonsei University College of Medicine, Seoul, Korea (the Republic of)

Correspondence to
Dr Hun-Mu Yang, Department of Anatomy, Yonsei University College of Medicine, Seodaemun-gu 03772, Korea (the Republic of); yanghm@yuhs.ac

T-HC and SHK are co-first authors.

Received 7 February 2021
Revised 19 April 2021
Accepted 21 April 2021

To cite: Cho T-H, Kim SH, O J, *et al*. *Reg Anesth Pain Med* Epub ahead of print: [*please include* Day Month Year]. doi:10.1136/rapm-2021-102588

ABSTRACT

Background A precise anatomical understanding of the thoracic paravertebral space (TPVS) is essential to understanding how an injection outside this space can result in paravertebral spread. Therefore, we aimed to clarify the three-dimensional (3D) structures of the TPVS and adjacent tissues using micro-CT, and investigate the potential routes for nerve blockade in this area.

Methods Eleven embalmed cadavers were used in this study. Micro-CT images of the TPVS were acquired after phosphotungstic acid preparation at the mid-thoracic region. The TPVS was examined meticulously based on its 3D topography.

Results Micro-CT images clearly showed the serial topography of the TPVS and its adjacent spaces. First, the TPVS was a very narrow space with the posterior intercostal vessels very close to the pleura. Second, the superior costotransverse ligament (SCTL) incompletely formed the posterior wall of the TPVS between the internal intercostal membrane and vertebral body. Third, the retro-SCTL space broadly communicated with the TPVS via slits, costotransverse space, intervertebral foramen, and erector spinae compartment. Fourth, the costotransverse space was intersegmentally connected to the adjacent retro-SCTL space.

Conclusions A non-destructive, multi-sectional approach using 3D micro-CT more comprehensively demonstrated the real topography of the intricate TPVS than previous cadaver studies. The posterior boundary and connectivity of the TPVS provides an anatomical rationale for the notion that paravertebral spread can be achieved with an injection outside this space.

INTRODUCTION

Thoracic paravertebral block is a well-established technique for regional anesthesia of the hemithorax in patients undergoing breast and thoracic surgeries.[1 2] However, there remains a potential risk of pneumothorax or unintentional neuraxial injection.[3 4] More superficial needle placement techniques with improved safety and feasibility, such as the erector spinae plane (ESP) block, have been introduced as potential alternatives to the conventional thoracic paravertebral block.[5 6] Recently, several approaches with a deeper target point than that for the ESP block, but not piercing the superior costotransverse ligament (SCTL), have been reported, with anatomical evidence of paravertebral spread and clinical effectiveness.[7–9]

The concept of the thoracic paravertebral space (TPVS) was shaped by clinical needs and has not been fully elucidated as a clearly delineated space from an anatomical perspective.[7] Specifically, although understanding its anatomy in terms of the posterior boundary and connectivity are crucial to understanding the action mechanism of recently descripted block techniques, there is a lack of detailed information regarding these points.

Manual dissection and histological observation are common methods in the investigation of human tissues. However, manual dissection can damage delicate structures during processing, and histological observation provides limited information through cross-sectional imaging. Micro-CT, as a non-destructive morphological method, is an effective tool for obtaining three-dimensional (3D) information with high resolution. Our previous studies using 3D micro-CT successfully demonstrated specific compartments within various complex structures of human tissue.[10–12]

Therefore, we aimed to clarify the 3D structures of the TPVS, and adjacent tissues using micro-CT and investigate the potential routes for nerve blockade in this area.

METHODS

Sample recruitment and dissection

A total of 11 embalmed cadavers (mean age: 82.8 years, 6 men and 5 women) were used for conventional dissection and micro-CT imaging analysis in this study. All cadavers had no deformity, trauma, and operative procedures in the thoracic spine region. Two experienced anatomists (T-HC and H-JK) dissected the thoracic spine region and examined the TPVS and its adjacent structures. Five cadavers were used to extensively investigate the TPVS and its adjacent structures using manual dissection. For micro-CT imaging, the TPVS tissue blocks of the T4-5 level were harvested from the six remaining cadavers. Conventional macroscopic examination and a 3D topographic analysis of the micro-CT images were performed to acquire following information: (1) 3D topography of the TPVS, including its detailed boundaries at the mid-thoracic level at the 4th and 5th rib levels; (2) the neurovascular contents within the TPVS and adjacent spaces; and (3) the spatial connections allowing intersegmental spreading between adjacent TPVSs. For one cadaver, a Venue Go ultrasound unit (GE

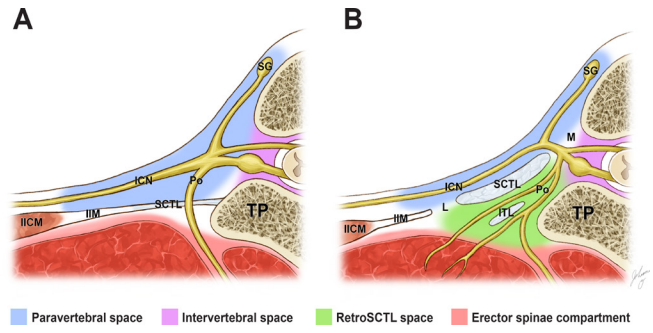

Figure 1 Territories of the thoracic paravertebral space (TPVS) based on the previous concept (A) and the present findings (B). The present findings show that the posterior border of the TPVS largely comprises the internal intercostal membrane (IIM) and superior costotransverse ligament (SCTL). The retro-SCTL space was partially open to the intervertebral foramen and directly connected to the TPVS via the medial and lateral slits (M and L, respectively). The posterior rami of the spinal nerve (Po) passed through the retro-SCTL space, proceeding toward the erector spinae compartment. ICN, intercostal nerve; IICM, internal intercostal muscle; ITL, intertransverse ligament; SG, sympathetic ganglion; TP, transverse process of vertebra.

Healthcare, Chicago, Illinois, USA) was used, with a high-frequency linear probe (L4-12t-RS, 4.2–13.0 MHz).

Micro-CT preparation with phosphotungstic acid and 3D visualization

Our micro-CT preparation technique for enhancing soft tissue contrast was used.[10–12] Briefly, to enhance the soft tissue contrast, TPVS tissue blocks were soaked in 1% phosphotungstic acid solution with 70% ethanol after serial dehydration (30%, 50%, and 70% for one night each). Micro-CT images were acquired using a micro-CT scanner (Skyscan 1173, Bruker, Kontich, Belgium), with a source voltage of 70 kV, source current of 114 μA, and image pixel of 20 μm^2. For a 3D visualization and analysis, the acquired section images were reconstructed using NRecon, CTVox (Bruker, Kontich, Belgium) and Mimics Research V.20.0 software (Materialise NV, Leuven, Belgium). Two representative 3D images of the TPVS are provided in online supplemental videos 1 and 2.

RESULTS

A total of 11 TPVS tissue blocks of the T4-5 level were finally analyzed using micro-CT imaging method in this study. The topography of the TPVS was very typical in all cases. Thus, the locations of the borders of the TPVS, connections among the spaces, and proceeding pattern of the spinal nerve branches can be described as follows.

Topography of the TPVS

There were several anatomical differences between the conventional TPVS concept (figure 1A) and the present study findings (figure 1B). The TPVS was vertically located at the intercostal levels. The posterior wall of the TPVS was mostly formed by the internal intercostal membrane and SCTL (figure 1B; online supplemental figure 5). The SCTL incompletely constituted a part of the posterior wall between the internal intercostal membrane and vertebral body (figure 2; online supplemental figure 1). In detail, the anterior layer of the SCTL ascended laterally and attached to the costal tubercle (figure 3; online supplemental figure 2). The SCTL was located very close to the pleura;

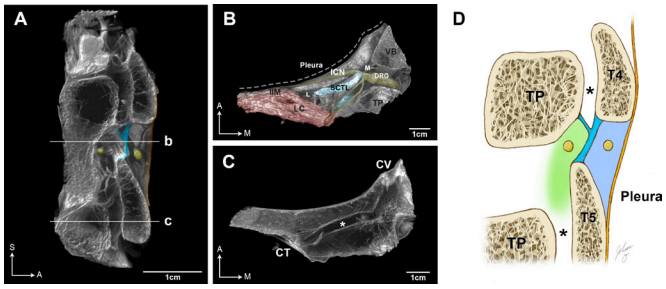

Figure 2 Micro-CT images of the thoracic paravertebral space (TPVS) at the mid-thoracic levels (4th and 5th ribs) in a sagittal section (A). Cross sections are shown at the levels of the TPVS (B) and the costotransverse space (C). An illustration (D) indicating the individual spaces on a sagittal section. The blueish and green colored regions indicate the TPVS and retro-superior costotransverse ligament (SCTL) space, respectively. The SCTL and intertransverse ligament are emphasized by blue coloring. The asterisks (*) indicate the costotransverse space. Uncolored raw micro-CT images are presented in online supplemental figure 1. A, anterior; CT, costotransverse joint; CV, costovertebral joint; DRG, dorsal root ganglion; ICN, intercostal nerve; IIM, internal intercostal membrane; L, lateral slit; LC, levatores costarum; M, medial slit; S, superior; TP, transverse process of vertebra; VB, vertebral body.

the mean distance between the pleura and the attachment of the SCTL was 7.8 mm (SD: 0.7 mm). Two slits in the SCTL were observed, located medially to costovertebral joint and laterally to the internal intercostal membrane (figures 2B and 3B; online supplemental figures 1B,2B and 5; online supplemental video 1).

Neurovascular bundles of the TPVS

The intervertebral foramina were located in a similar anteroposterior position, or anterior to the SCTL. Although the nomenclature, "para"vertebral, indicates that this space might mostly comprise the nervous component of the spinal nerve, the intervertebral foramen did not completely open to the TPVS. Instead, the medial base of the TPVS was mostly formed by the vertebral body. Only the anterior rami of the spinal nerve and sympathetic trunk emerged at the TPVS and the posterior rami of the spinal nerve directly proceeded into the space posterior to the SCTL and erector spinae compartment. Especially, the intercostal nerves entered the TPVS directly via the medial slit (figure 2B;

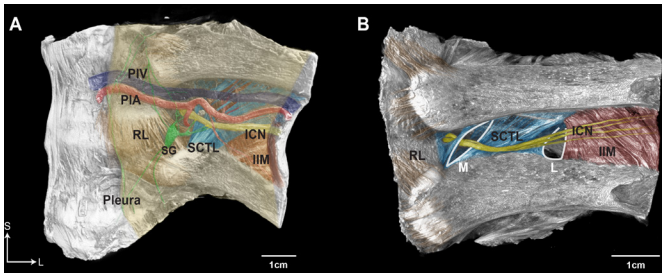

Figure 3 Posterior intercostal artery (PIA) and posterior intercostal vein (PIV), and intercostal nerve (ICN), within the thoracic paravertebral space (TPVS) are shown. The neurovascular bundle located beneath the pleura is shown (A). The medial and lateral slits (M and L, respectively) are clearly revealed after removal of the pleura and vessels (B). Uncolored raw micro-CT images are presented in online supplemental figure 2. IIM, internal intercostal membrane; L, lateral; RL, radiate ligament of the costovertebral joint; S, superior; SCTL, superior costotransverse ligament; SG, sympathetic ganglion.

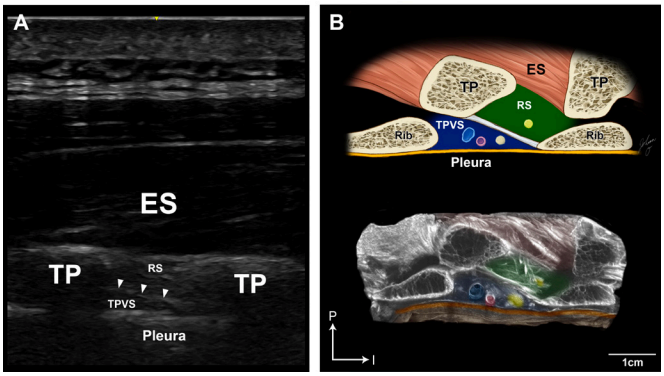

Figure 4 Comparison between an ultrasound image (A) and the corresponding micro-CT image (B) of the thoracic paravertebral space (TPVS) and retro-superior costotransverse ligament (SCTL) space (RS). Arrowheads indicate the SCTL. The posterior intercostal artery and vein, and intercostal nerve (colored as red, blue, and yellow, respectively), are clearly observable only on the micro-CT image. The posterior rami of the spinal nerve passed through the retro-SCTL space, proceeding toward the erector spinae compartment (ES). Uncolored raw micro-CT images are presented in online supplemental figure 3. I, inferior; P, posterior; TP, transverse process of vertebra.

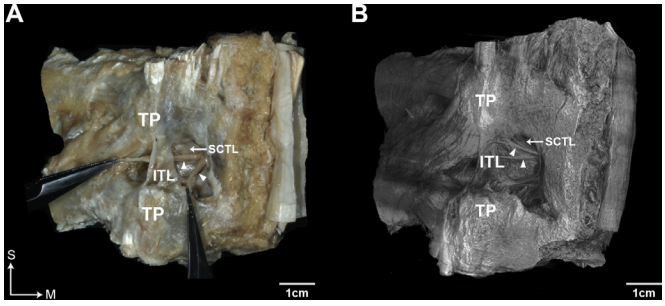

Figure 5 Intertransverse ligament (ITL) and the posterior rami of the spinal nerve in dissection (A) and micro-CT (B) image, viewed from behind. Arrowheads indicate the twigs of the posterior rami of the spinal nerve. M, medial; S, superior; SCTL, superior costotransverse ligament; TP, transverse process of vertebra.

online supplemental figure 1B) or indirectly after piercing the SCTL (figure 3B; online supplemental figure 2B). The sympathetic trunk was located within the TPVS, beneath the pleura (figure 3A; online supplemental figure 2A). Very tiny fibers of white and gray communicantes connected between the trunk and anterior rami within the TPVS.

The vessels within the TPVS were observed as very close to the pleura (figures 3A and 4B; online supplemental figures 2A and 3; online supplemental video 2). The posterior intercostal artery entered the TPVS, and its branch proceeded through the lateral slit after a bifurcation on the SCTL. The posterior intercostal artery was accompanied by the posterior intercostal vein at its upper location. The posterior intercostal vessels continued laterally within the TPVS, beneath the pleura, midway between adjacent ribs (online supplemental video 2).

Retro-SCTL space

We observed a potential spreading space, which we termed "retro-SCTL space," broadly connecting to the TPVS, intervertebral foramen, and erector spinae compartment (online supplemental video 1). Previously, the space posterior to the SCTL was considered a part of the retrolaminar space, preserving the erector spinae compartment (figure 1A). However, this retro-SCTL space was not situated at the retrolaminar (behind the lamina of the vertebra) position (figure 2B; online supplemental figure 1B). Although it was a continuum of the erector spinae compartment, there was only loose connective tissue in the retro-SCTL space (online supplemental figure 4). This space was partially open to the intervertebral foramen and directly connected to the TPVS via the medial and lateral slits of SCTL. The intercostal membrane was partially merged with the levatores costarum at the lateral slit position. The posterior rami of the spinal nerve passed through the retro-SCTL space, proceeding toward the erector spinae compartment. Moreover, the proximal part of the anterior rami was situated in this space.

The ultrasound image of the posterior thoracic region corresponded to the micro-CT sagittal image (figure 4; online supplemental figure 3). On ultrasound, the SCTL demarcating the boundaries between the TPVS and retro-SCTL space could be distinguished, and there was an intensity difference between the retro-SCTL space and erector spinae compartment.

Costotransverse space

A topographic conduit for vertical spreading was clearly verified in the present study. It was previously known that there was ligamentous tissue (costotransverse ligament) between the rib and transverse process. However, in the present study, this costotransverse space was very clear, comprizing loose connective and adipose tissues, with a width of 3.1 mm (SD: 1.1 mm) (figure 2C; online supplemental figure 1C; online supplemental videos 1 and 2). The costotransverse space seemed to provide a distinct conduit between adjacent TPVS and retro-SCTL spaces.

Some fibers of the SCTL (previously known as the posterior lamina or layer) crossed the retro-SCTL space and attached to the lower surface of the transverse process (figure 2A). Thus, the SCTL formed an incomplete ligamentous barrier between the retro-SCTL space or the TPVS and the costotransverse space.

Interligamentary space between the SCTL and intertransverse ligament (ITL)

At the retro-SCTL space, the ITL was located posterior to the SCTL (figure 5). The ITL was a narrow distinct ligament that attached to adjacent tubercles. The ITL was distinctly separated from the SCTL; thus, there was a distinct interligamentary space between them. Some twigs of the posterior rami of the spinal nerve passed through this space and proceeded laterally.

DISCUSSION

The current study examined the 3D topography of the TPVS and revealed more specific information regarding its anatomy. The posterior border of the TPVS was incompletely formed by the SCTL and, in all cases, the SCTL had slits that were connected with the TPVS. The retro-SCTL space contained the posterior rami of the spinal nerve and broadly connected to the TPVS via the slits of the SCTL, costotransverse space, intervertebral foramen, and erector spinae compartment.

The posterior boundary and connectivity of the TPVS have clinical significance for nerve blockade in this space. Our study confirms that anatomically the TPVS is not an entirely closed space, and its posterior boundary does not comprise a simple structure. In fact, this finding was already described in previously published studies, although conclusive anatomical evidence has not been sufficient. There have been many anatomical illustrations describing this space so far. Among

them, a previous illustration of the TPVS by Boezaart *et al*[1 2] included all of our current findings. The internal intercostal membrane largely constituted the posterior border of the TPVS, along with the rib and SCTL. This finding suggests permeability to the TPVS, as well as the volume of the TPVS itself, which seems to be considerably changeable in human subjects, with dynamic respiratory movement. The SCTL is the obvious barrier that must be passed to spread to the TPVS. The SCTL was a distinctly robust ligament, which may restrict injectate spread, but the slits at the medial and lateral ends can act as channels to the TPVS, as shown in the current study. The retro-SCTL space, between the SCTL and erector spinae compartment, is not an empty space, but is filled with muscles, adipose, and loose connective tissue complexes. This space was previously described in a valid study by Krediet *et al*[13] along with histological findings. Our 3D micro-CT imaging demonstrated that this space contains the posterior rami of the spinal nerve, and the proximal part of the anterior rami was situated in this space. Additionally, this space was partially open to the intervertebral foramen and directly connected to TPVS via the medial and lateral slits of the SCTL. Moreover, the costotransverse space vertically provides a potential conduit between the retro-SCTL space and the TPVS at adjacent levels.

The present study findings suggest the retro-SCTL space as a potential space for paravertebral spread. Indeed, this space has been described as a new target space in several recent studies.[7–9] Using the midpoint transverse process to the pleura block has been shown to result in extensive paravertebral spread with sympathetic chain involvement, and has demonstrated successful postoperative analgesia in breast surgical procedures.[7] Also, pleural displacement and ESP spread have been observed under real-time ultrasonography.[7] The costotransverse block, comprizing an injection into the thoracic intertransverse tissue complex located posterior to the SCTL, has shown paravertebral spread, with anterior rami and sympathetic trunk involvement, comparable to that with conventional paravertebral block in cadavers.[8] Recent reports have described a similar approach, comprizing a local anesthetic injection to the anterior region of the ITL, immediately posterior to the junction of the SCTL and cranial transverse process.[9] Despite a limited sample size, this technique resulted in good analgesic efficacy in patients who underwent breast surgery or thoracotomy.[9 14] Although the above mentioned reports used slightly different anatomical nomenclatures, block names, and needle trajectories, the final target space seem to be identical to the retro-SCTL space.

The ESP block targets the fascial plane deep to the erector spinae muscle at the tip of the transverse process[5]; thus, there are no doubts about its safety when compared with the conventional paravertebral block. Additionally, clinical reports support the effectiveness of the ESP block, and even its analgesic effect on visceral pain.[15–17] In contrast, human cadaver studies revealed limited, or even no, paravertebral spread in the ESP block, accompanied with more predominantly posterior back muscle or fascia spread.[8 18 19] It is uncertain whether ESP block and blocks targeting the retro-SCTL space can replace the conventional paravertebral block. It may be reasonable to assume that these approaches differ in terms of their specific clinical indications and risk–benefit ratio. Regarding paravertebral spread, our results suggest that an injection into the retro-SCTL space, which has more potential pathways to the TPVS, may be anatomically more advantageous than an ESP injection. However, there is currently a lack of clinical information about the effectiveness of retro-SCTL space blocks. Thus, the significance of our results should be evaluated by clinical comparisons, especially in patient subgroups requiring anterior thoracic area coverage.

Herein, thorough and reliable 3D information of the TPVS region was provided using high-resolution micro-CT images. However, the current study has inevitable limitations as an anatomical study using cadavers, in which dimensional changes in the space due to the respiration cycle and the real-time spreading pattern of the injectate could not be validated. In the current study, we intensively examined the mid-thoracic region; comparative topography at other vertebral levels might be elucidated in a subsequent cadaveric study. Also, further study is needed to determine if there is individual variation of the TPVS due to physical factors such as height and weight.

In conclusion, the 3D topography of the posterior boundary and connectivity of the TPVS provides an anatomical rationale supporting the notion that paravertebral spread may be achieved with an injection outside the TPVS. In particular, our results suggest that controlled clinical studies are needed to verify the retro-SCTL space as a target space for neural blockade in the thoracic region.

Correction notice This article has been corrected since it published Online First. The corresponding author's ORCID ID has been corrected.

Acknowledgements We are grateful to the people who very nobly donated their bodies to the Surgical Anatomy Education Centre at the Yonsei University College of Medicine. Additionally, the authors wish to thank Jun Ho Kim, Jong Ho Bang, and Tae-Jun Ha for their technical support (all are staff members of the Surgical Anatomy Education Centre at the Yonsei University College of Medicine). One of the authors (JO) produced the illustrations in all figures.

Contributors T-HC and SHK (these authors contributed equally to this work): dissection, experiment, validation, formal analysis, writing and editing of the original manuscript. JO: data curation, three-dimensional (3D) images analysis and figure illustrations. H-JK: dissection, experiment, and 3D images analysis. KWK: experiment, data curation, and formal analysis. H-MY: project administration, conceptualization, design, supervision, formal analysis, and critical revision of the manuscript for intellectual content. All authors read and gave final approval of the version to be published.

Funding This work was supported by the National Research Foundation of Korea grant funded by the Korea government (MSIT) (No. 2020R1F1A1058123). No other external funding or competing interests declared.

Competing interests None declared.

Patient consent for publication Not required.

Ethics approval The Institutional Review Board approved the study for exemption from formal review (No. 4-2020-0997). All cadavers were legally donated to the Surgical Anatomy Education Centre at Yonsei University College of Medicine (No. 21-001).

Provenance and peer review Not commissioned; externally peer reviewed.

Data availability statement Data are available upon reasonable request. Deidentified data will be made available upon reasonable written request submitted to the corresponding author.

ORCID iDs
Shin Hyung Kim http://orcid.org/0000-0003-4058-7697
Ki Wook Kim http://orcid.org/0000-0003-0630-3881
Hun-Mu Yang http://orcid.org/0000-0003-1954-0114

REFERENCES

1 Boezaart AP, Raw RM. Continuous thoracic paravertebral block for major breast surgery. *Reg Anesth Pain Med* 2006;31:470–6.
2 Boezaart AP, Lucas SD, Elliott CE. Paravertebral block: cervical, thoracic, lumbar, and sacral. *Curr Opin Anaesthesiol* 2009;22:637–43.
3 Pace MM, Sharma B, Anderson-Dam J, *et al*. Ultrasound-Guided thoracic paravertebral blockade: a retrospective study of the incidence of complications. *Anesth Analg* 2016;122:1186–91.
4 Kus A, Gurkan Y, Gul Akgul A, *et al*. Pleural puncture and intrathoracic catheter placement during ultrasound guided paravertebral block. *J Cardiothorac Vasc Anesth* 2013;27:e11–12.

5 Forero M, Adhikary SD, Lopez H, *et al*. The erector spinae plane block: a novel analgesic technique in thoracic neuropathic pain. *Reg Anesth Pain Med* 2016;41:621–7.
6 El-Boghdadly K, Pawa A. The erector spinae plane block: plane and simple. *Anaesthesia* 2017;72:434–8.
7 Costache I, de Neumann L, Ramnanan CJ, *et al*. The mid-point transverse process to pleura (MTP) block: a new end-point for thoracic paravertebral block. *Anaesthesia* 2017;72:1230–6.
8 Nielsen MV, Moriggl B, Hoermann R, *et al*. Are single-injection erector spinae plane block and multiple-injection costotransverse block equivalent to thoracic paravertebral block? *Acta Anaesthesiol Scand* 2019;63:1231–8.
9 Kilicaslan A, Sarkilar G, Altınok T, *et al*. A novel ultrasound-guided technique in peri-paravertebral area: Subtransverse process interligamentary (Stil) plane block: the game has not ended yet. *J Clin Anesth* 2020;60:76–7.
10 O J, Kwon H-J, Kim SH, *et al*. Use of micro X-ray computed tomography with phosphotungstic acid preparation to visualize human fibromuscular tissue. *J Vis Exp* 2019. doi:10.3791/59752. [Epub ahead of print: 05 09 2019].
11 Kwon H-J, O J, Cho T-H, *et al*. The nasolabial fold: a Micro-Computed tomography study. *Plast Reconstr Surg* 2020;145:71–9.
12 O J, Kwon H-J, Choi Y-J, *et al*. Three-Dimensional structure of the orbicularis retaining ligament: an anatomical study using micro-computed tomography. *Sci Rep* 2018;8:17042.
13 Krediet AC, Moayeri N, van Geffen G-J, *et al*. Different approaches to ultrasound-guided thoracic paravertebral block: an illustrated review. *Anesthesiology* 2015;123:459–74.
14 Ince I, Dostbil A, Ozmen O, *et al*. Subtransverse process interligamentary (Stil) plane block for postoperative pain management after breast surgery. *J Clin Anesth* 2020;61:109649.
15 Chin KJ, Malhas L, Perlas A. The erector spinae plane block provides visceral abdominal analgesia in bariatric surgery: a report of 3 cases. *Reg Anesth Pain Med* 2017;42:372–6.
16 Bang S, Chung J, Kwon W, *et al*. Erector spinae plane block for multimodal analgesia after wide midline laparotomy: a case report. *Medicine* 2019;98:e15654.
17 Kwon H-M, Kim D-H, Jeong S-M, *et al*. Does erector spinae plane block have a visceral analgesic effect?: a randomized controlled trial. *Sci Rep* 2020;10:8389.
18 Yang H-M, Choi YJ, Kwon H-J, *et al*. Comparison of injectate spread and nerve involvement between retrolaminar and erector spinae plane blocks in the thoracic region: a cadaveric study. *Anaesthesia* 2018;73:1244–50.
19 Ivanusic J, Konishi Y, Barrington MJ. A cadaveric study investigating the mechanism of action of erector spinae blockade. *Reg Anesth Pain Med* 2018;43:567–71.

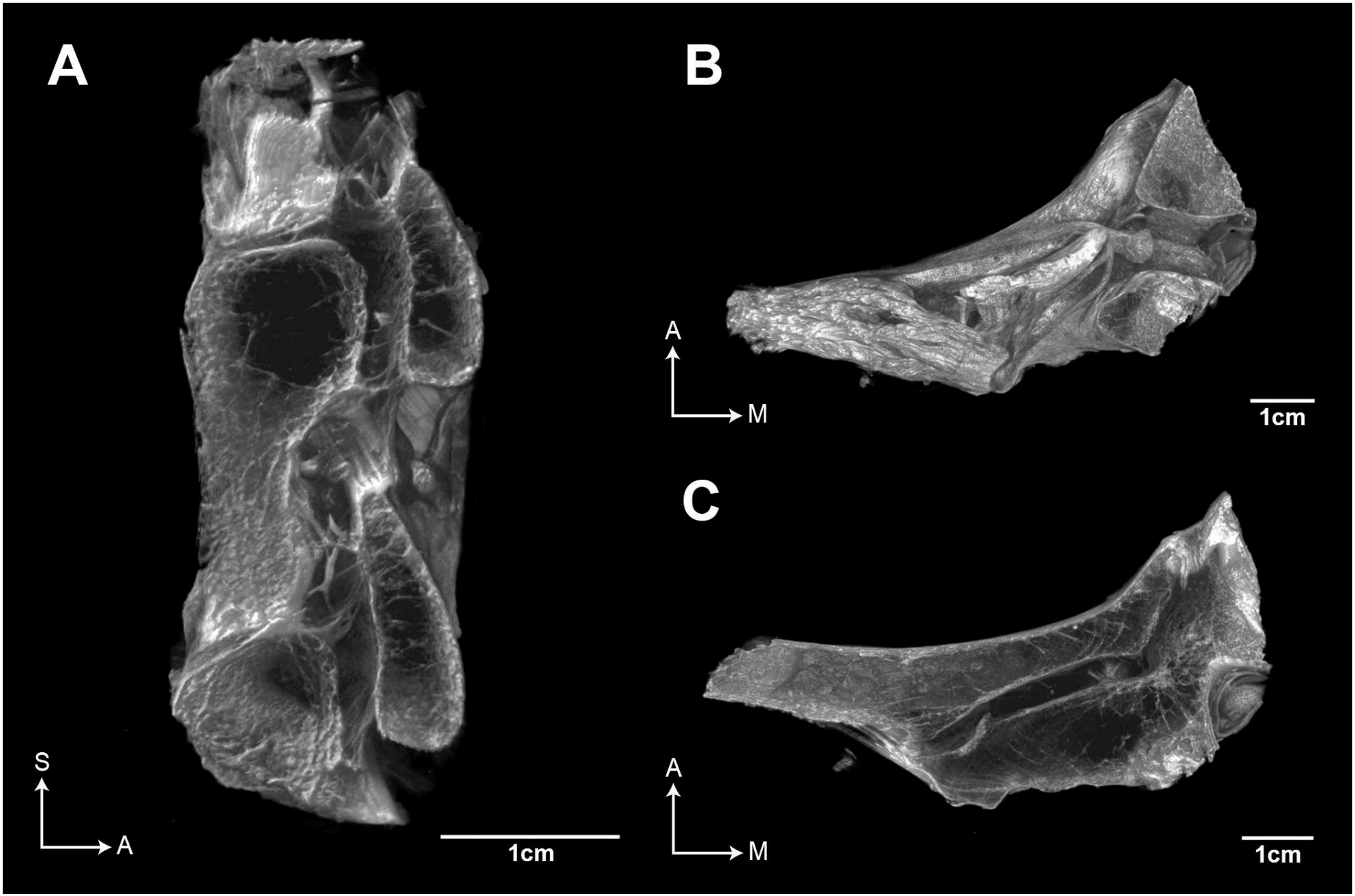
A
S
A
1cm
B
A
M
1cm
C
A
M
1cm

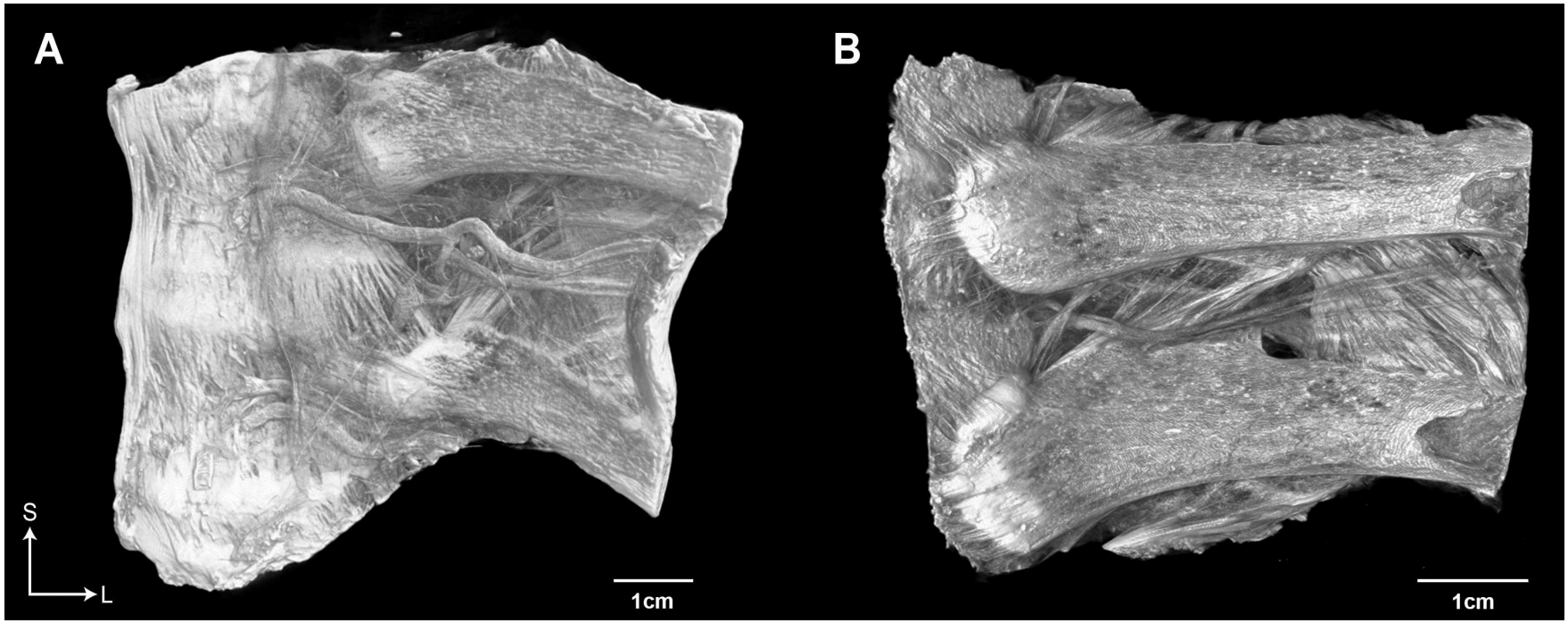
A
B
S
L
1cm
1cm

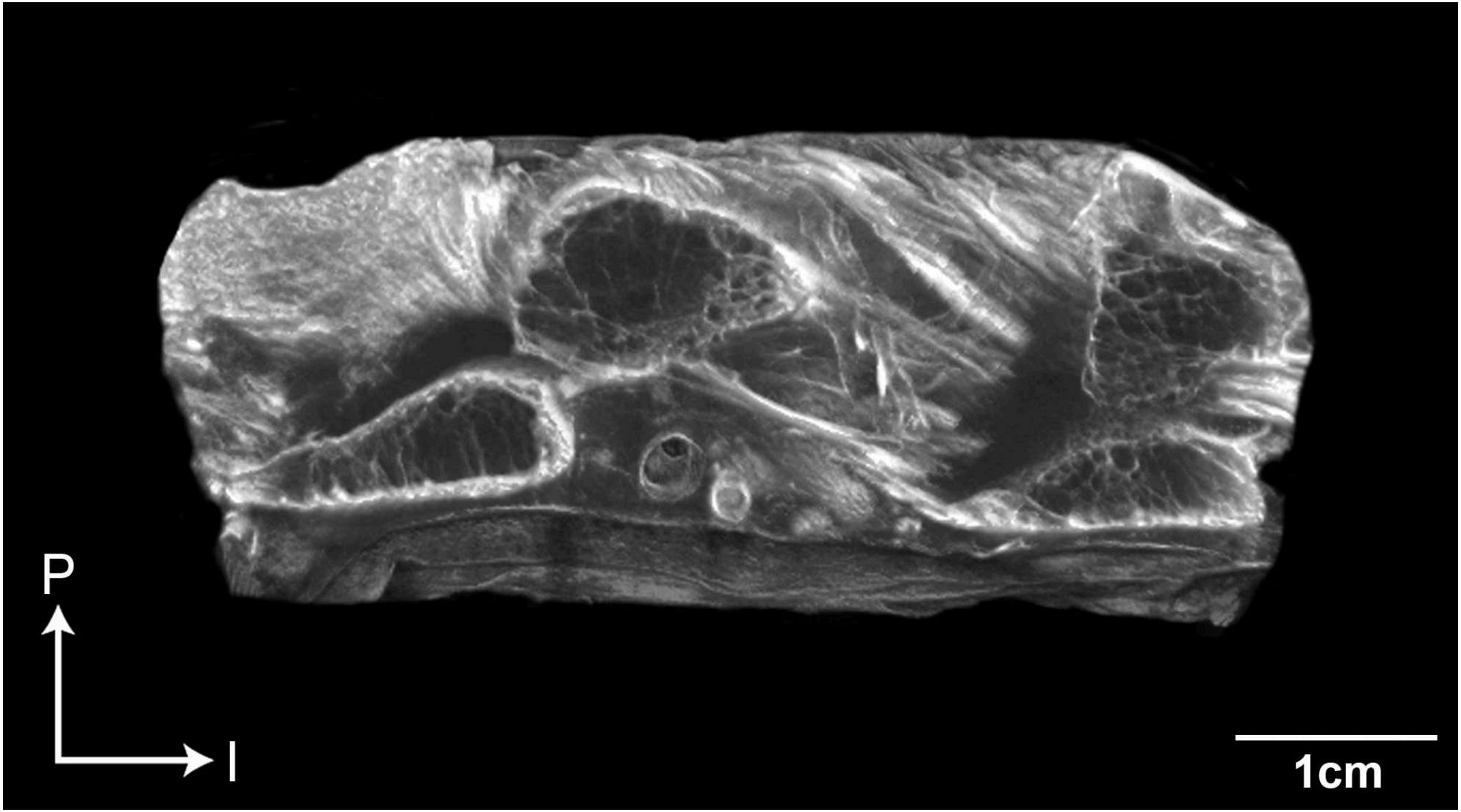
P
I
1cm

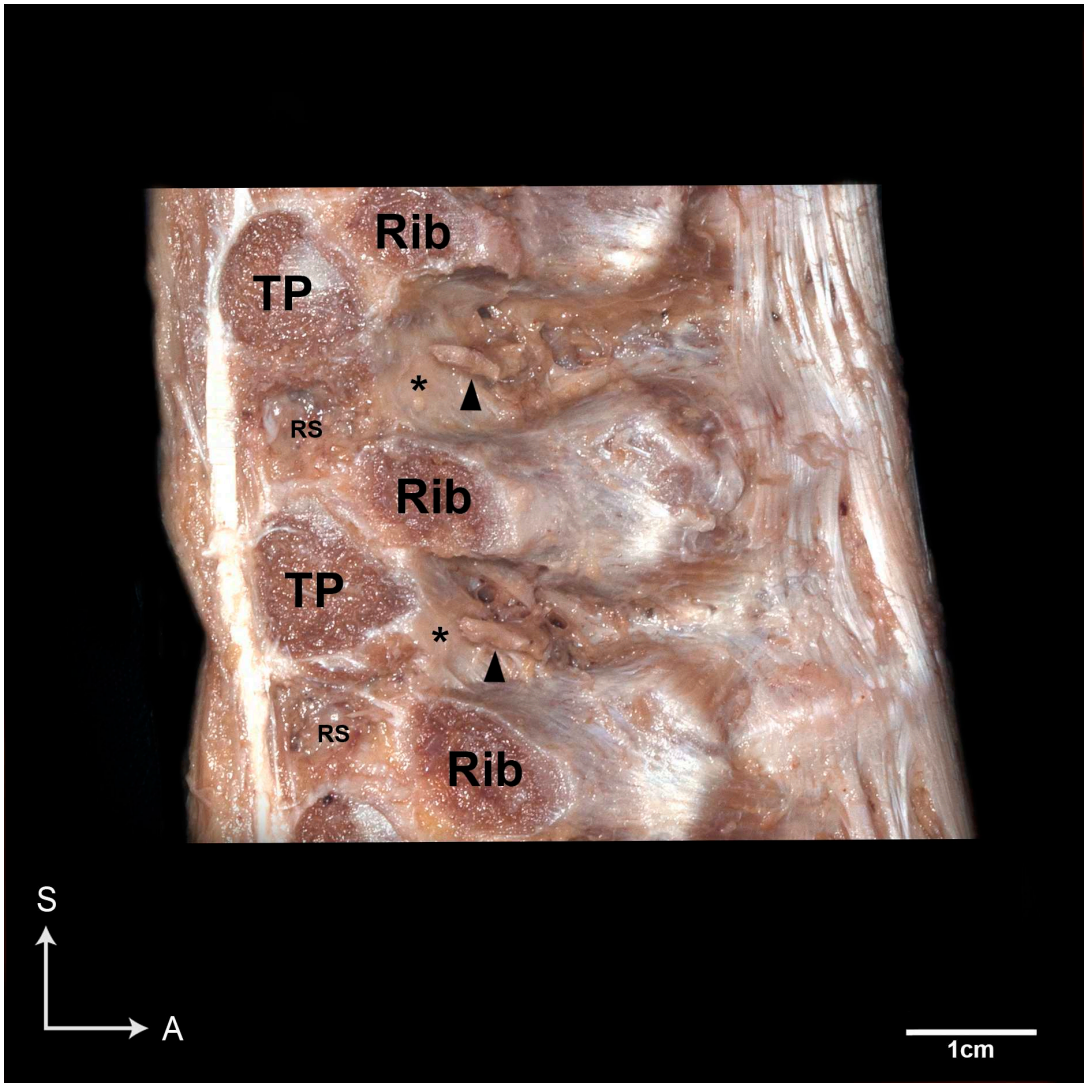
Rib
TP
*
RS
Rib
TP
*
RS
Rib
S
A
1cm

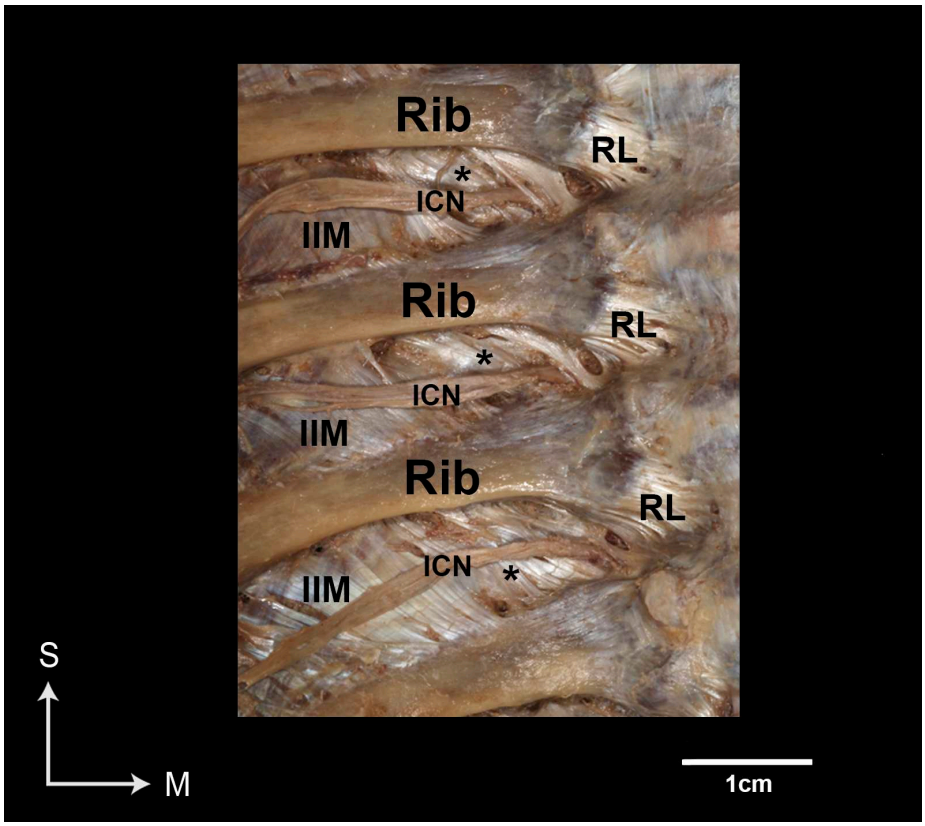
Rib
RL
*
ICN
IIM
Rib
RL
*
ICN
IIM
Rib
RL
ICN
*
IIM
S
M
1cm

Online supplemental material legends

Online supplemental video 1. Three-dimensional images of the thoracic paravertebral space (TPVS) are shown in sagittal (0:00-0:12) and cross (0:14-0:25) sections.

The pleura and vessels are removed for a clear visualization of the superior costotransverse ligament (SCTL) and intercostal nerve (ICN). Sections are presented from medial to lateral regions in the sagittal section and from superior to inferior regions in the cross-section.

In the sagittal section, the SCTL is observed to separate the TPVS from the retro-SCTL space (RS) (0:03). There were medial (0:03) and lateral (0:08) slits, and the ICN passes through the medial slit (0:03). The costotransverse space (CTS) is clearly observed at the upper level (0:17) of the TPVS. The medial and distal slits (M and L, respectively) adjacent to the SCTL are also clearly recognized in the cross-section (0:22).

Abbreviations: A, anterior; DRG, dorsal root ganglion; ITL, intertransverse ligament; IIM, internal intercostal membrane; LC, levatores costarum; S, superior; L, lateral.

Online supplemental video 2. Three-dimensional images of the posterior intercostal artery and vein (PIA and PIV, respectively) within the thoracic paravertebral space (TPVS) are shown in sagittal (0:02-0:13) and cross (0:16-0:28) sections.

The PIA and PIV proceed laterally between the vertebral body and pleura (0:04-0:08), and then enter the TPVS (0:08-0:12). At the intercostal space, the PIV and PIA are situated at the middle 1/3 level. The cross-section provides a clear view of the pathway of the PIV (0:23) and PIA (0:25) at the TPVS.

Abbreviations: SCTL, superior costotransverse ligament; ICN, intercostal nerve; S, superior; L, lateral; A, anterior.

Cho T-H, *et al. Reg Anesth Pain Med* 2021;0:1–5. doi: 10.1136/rapm-2021-102588

Online supplemental figure 1. Raw images (uncoloured) of micro-computed tomography images are shown (corresponding to figures 2A, 2B and 2C)

Abbreviations: S, superior; A, anterior; M, medial.

Online supplemental figure 2. Raw images (uncoloured) of micro-computed tomography images are shown (corresponding to figures 3A and 3B)

Abbreviations: S, superior; L, lateral.

Online supplemental figure 3. Raw images (uncoloured) of micro-computed tomography images are shown (corresponding to figure 4B)

Abbreviations: P, posterior; I, inferior.

Online supplemental figure 4. A sagittal section (from a cadaver) of the mid-thoracic region is shown. Arrowheads indicate the intercostal nerve. The asterisks (*) indicate the superior costotransverse ligament (SCTL).

Abbreviations: TP, transverse process; RS, retro-SCTL space; S, superior; A, anterior.

Online supplemental figure 5. A dissected specimen of the mid-thoracic region of a cadaver is shown. The internal intercostal membrane (IIM) is a connective tissue fiber strongly oriented with the superior costotransverse ligament (*).

Abbreviations: ICN, intercostal nerve; RL, radiate ligament of the costovertebral joint; S, superior; M, medial.

Cho T-H, *et al. Reg Anesth Pain Med* 2021;0:1–5. doi: 10.1136/rapm-2021-102588

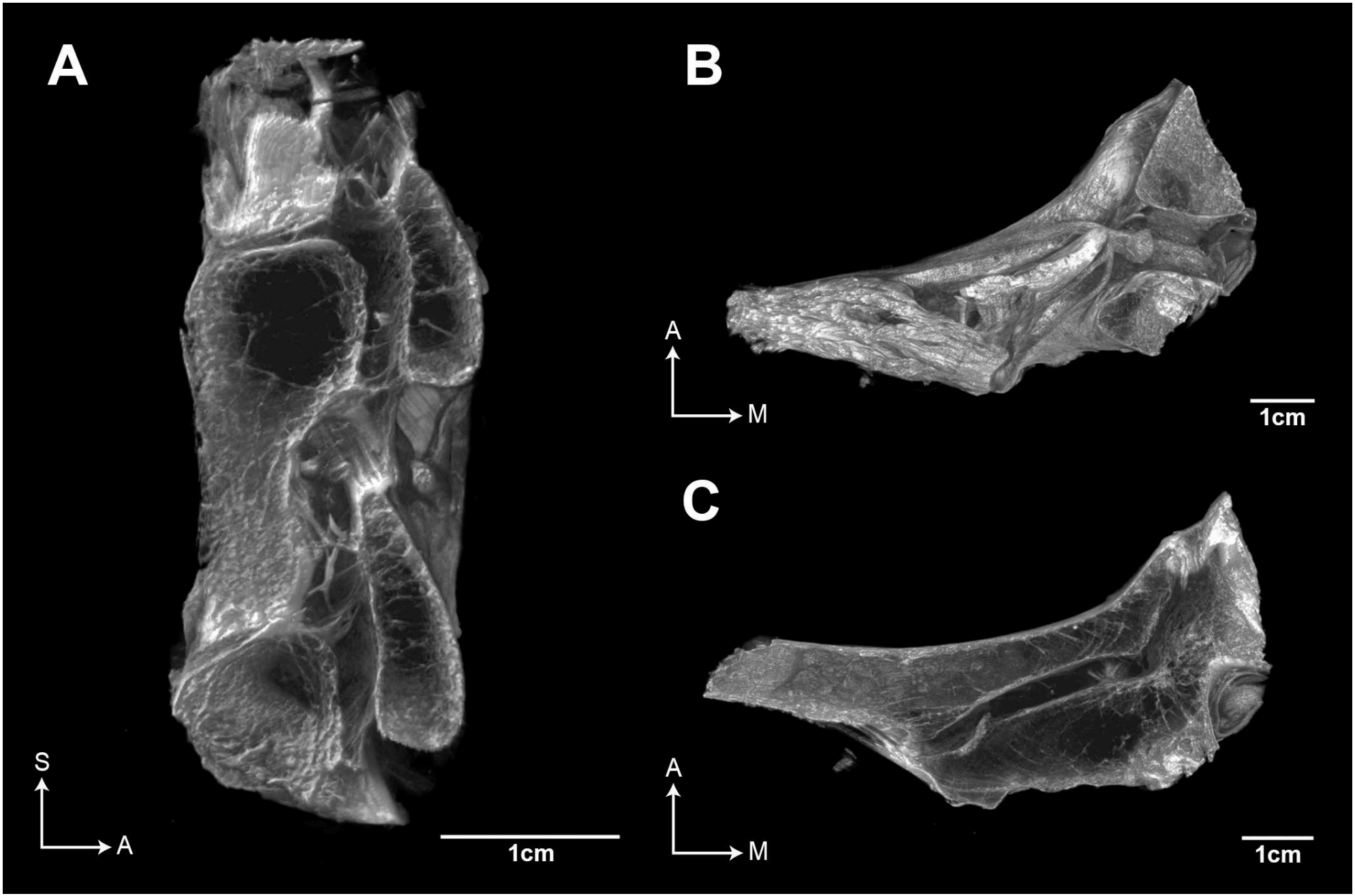
A
S
A
1cm
B
A
M
1cm
C
A
M
1cm

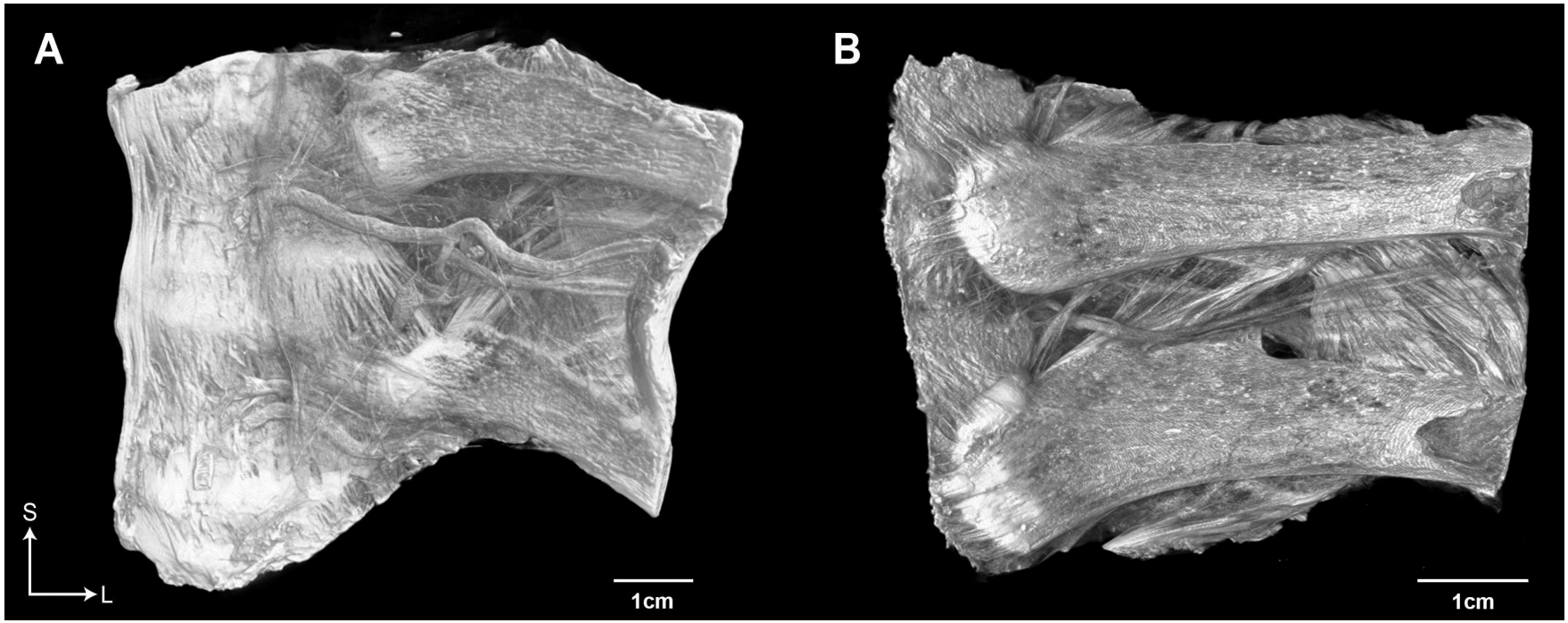
A
B
S
L
1cm
1cm

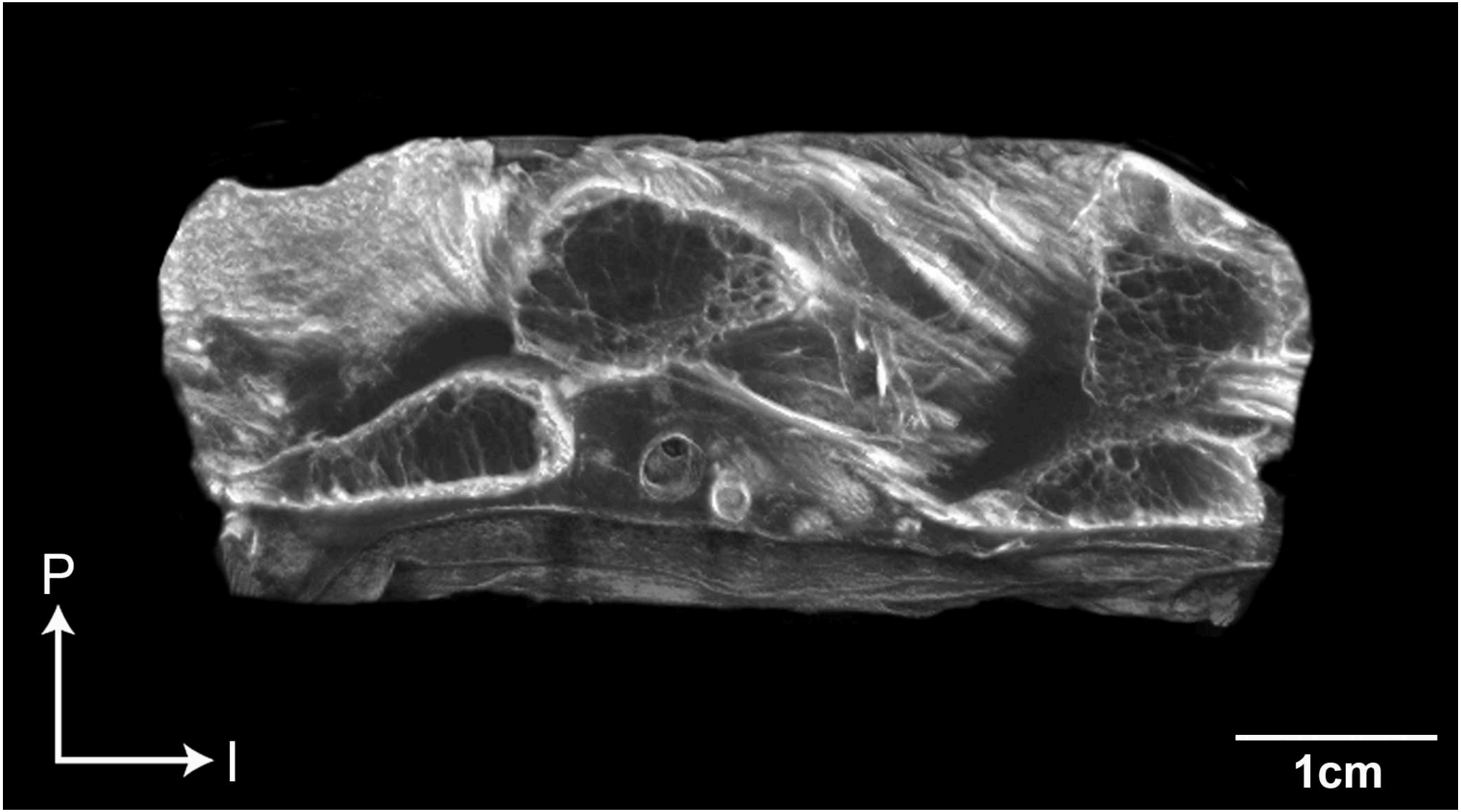
P
I
1cm

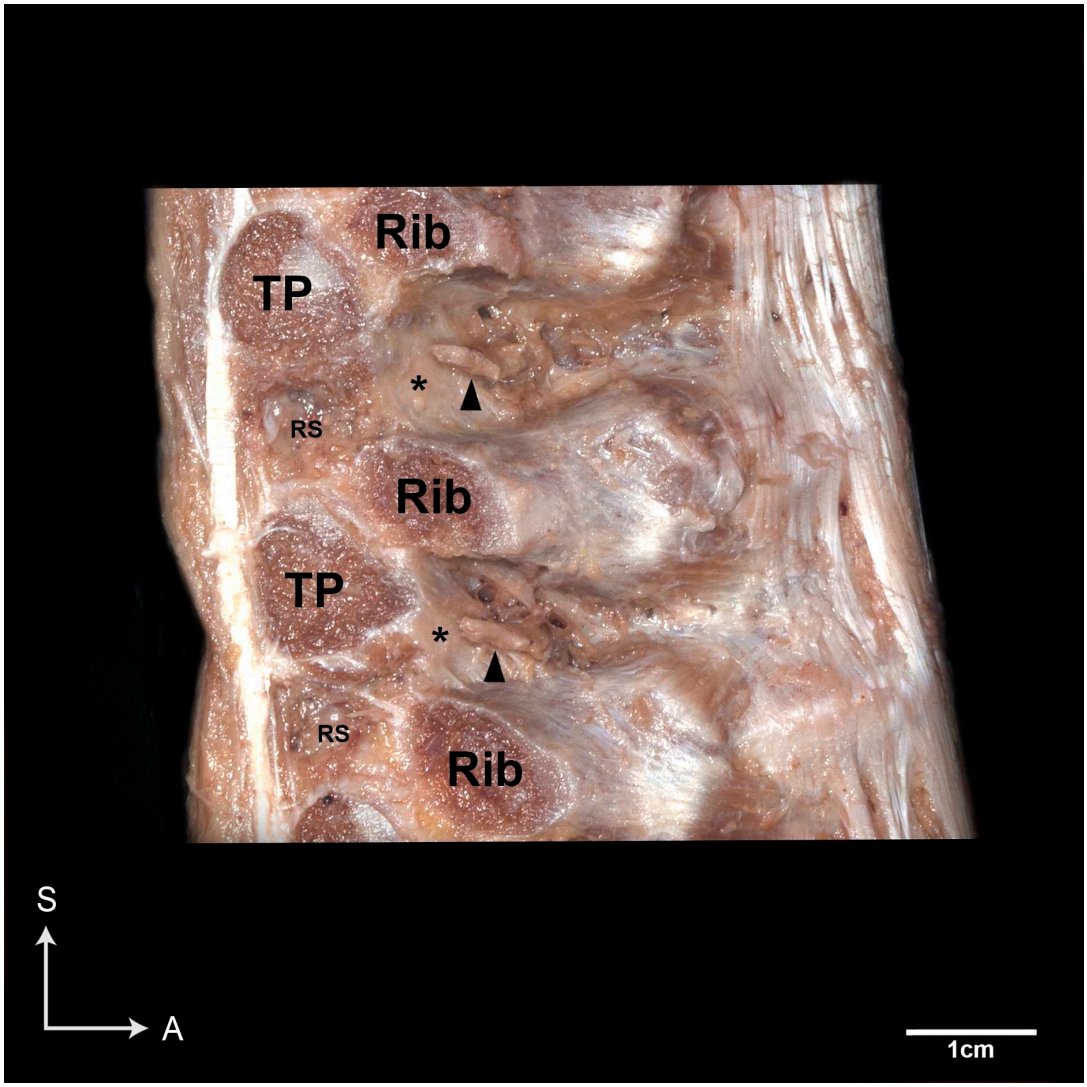
Rib
TP
*
RS
Rib
TP
*
RS
Rib
S
A
1cm

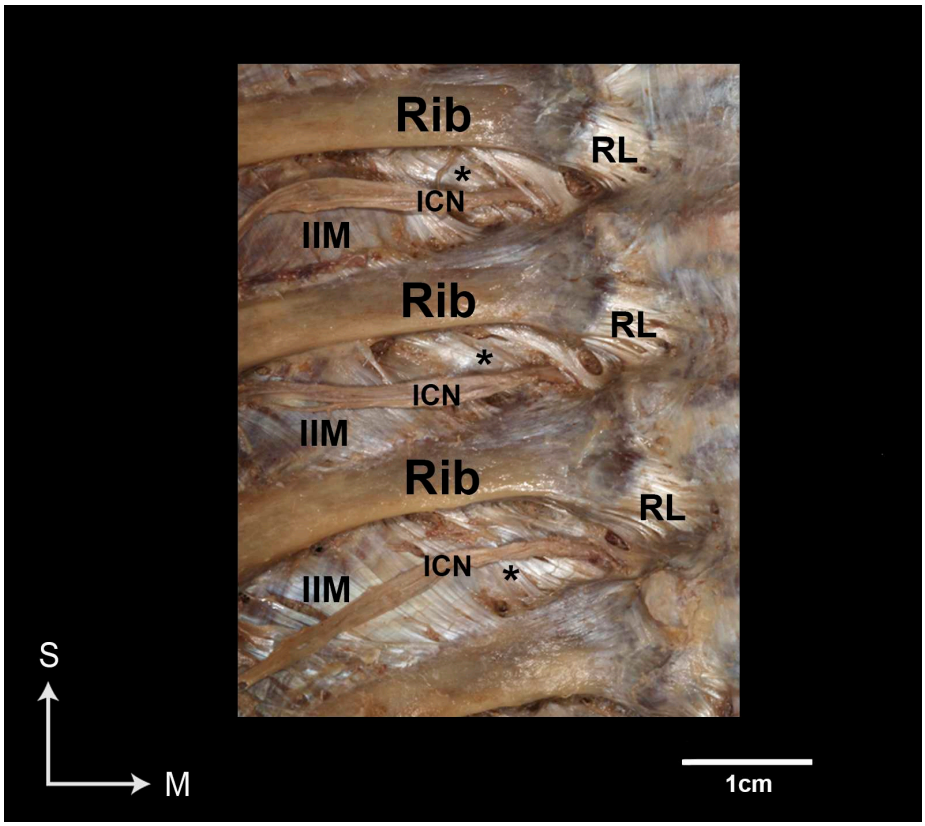
Rib
RL
*
ICN
IIM
Rib
RL
*
ICN
IIM
Rib
RL
ICN
*
IIM
S
M
1cm

Online supplemental material legends

Online supplemental video 1. Three-dimensional images of the thoracic paravertebral space (TPVS) are shown in sagittal (0:00-0:12) and cross (0:14-0:25) sections.

The pleura and vessels are removed for a clear visualization of the superior costotransverse ligament (SCTL) and intercostal nerve (ICN). Sections are presented from medial to lateral regions in the sagittal section and from superior to inferior regions in the cross-section.

In the sagittal section, the SCTL is observed to separate the TPVS from the retro-SCTL space (RS) (0:03). There were medial (0:03) and lateral (0:08) slits, and the ICN passes through the medial slit (0:03). The costotransverse space (CTS) is clearly observed at the upper level (0:17) of the TPVS. The medial and distal slits (M and L, respectively) adjacent to the SCTL are also clearly recognized in the cross-section (0:22).

Abbreviations: A, anterior; DRG, dorsal root ganglion; ITL, intertransverse ligament; IIM, internal intercostal membrane; LC, levatores costarum; S, superior; L, lateral.

Online supplemental video 2. Three-dimensional images of the posterior intercostal artery and vein (PIA and PIV, respectively) within the thoracic paravertebral space (TPVS) are shown in sagittal (0:02-0:13) and cross (0:16-0:28) sections.

The PIA and PIV proceed laterally between the vertebral body and pleura (0:04-0:08), and then enter the TPVS (0:08-0:12). At the intercostal space, the PIV and PIA are situated at the middle 1/3 level. The cross-section provides a clear view of the pathway of the PIV (0:23) and PIA (0:25) at the TPVS.

Abbreviations: SCTL, superior costotransverse ligament; ICN, intercostal nerve; S, superior; L, lateral; A, anterior.

Cho T-H, *et al. Reg Anesth Pain Med* 2021;0:1–5. doi: 10.1136/rapm-2021-102588

Online supplemental figure 1. Raw images (uncoloured) of micro-computed tomography images are shown (corresponding to figures 2A, 2B and 2C)

Abbreviations: S, superior; A, anterior; M, medial.

Online supplemental figure 2. Raw images (uncoloured) of micro-computed tomography images are shown (corresponding to figures 3A and 3B)

Abbreviations: S, superior; L, lateral.

Online supplemental figure 3. Raw images (uncoloured) of micro-computed tomography images are shown (corresponding to figure 4B)

Abbreviations: P, posterior; I, inferior.

Online supplemental figure 4. A sagittal section (from a cadaver) of the mid-thoracic region is shown. Arrowheads indicate the intercostal nerve. The asterisks (*) indicate the superior costotransverse ligament (SCTL).

Abbreviations: TP, transverse process; RS, retro-SCTL space; S, superior; A, anterior.

Online supplemental figure 5. A dissected specimen of the mid-thoracic region of a cadaver is shown. The internal intercostal membrane (IIM) is a connective tissue fiber strongly oriented with the superior costotransverse ligament (*).

Abbreviations: ICN, intercostal nerve; RL, radiate ligament of the costovertebral joint; S, superior; M, medial.

Cho T-H, *et al. Reg Anesth Pain Med* 2021;0:1–5. doi: 10.1136/rapm-2021-102588